

Performance of a PPM hard decision-based ARQ-FSO system in a weak turbulence channel

Jianjun Yin (尹建军), Hongzhan Liu (刘宏展)*, Rong Huang (黄蓉),
Zhengguang Gao (高争光), and Zhongchao Wei (韦中超)

Guangdong Provincial Key Laboratory of Nanophotonic Functional Materials and Devices, South China Normal University, Guangzhou 510006, China

*Corresponding author: lhzscnu@163.com

Received October 8, 2016; accepted February 24, 2017; posted online March 16, 2017

We present an automatic repeat request (ARQ) free space optical (FSO) system, which consists of a pulse position modulation (PPM) hard decision and an ARQ. The new ARQ's data error detection is based on a PPM hard decision's results and can eliminate the traditional ARQ information redundancy. The results of the numerical simulation have a good agreement with theoretical analysis and show that the ARQ-FSO system can effectively improve the bit error rate (BER) performance of the direct hard decision PPM system. Additionally, the proposed system significantly improves the average throughput efficiency compared to traditional ARQ systems. These characteristics make the ARQ-FSO system suitable for application in low BER and complexity FSO scenarios.

OCIS codes: 010.1300, 010.1330, 060.2605.

doi: 10.3788/COL201715.060101.

In recent years, free space optical (FSO) communication has drawn noticeable attention, owing to its high transmission rate, high bandwidth, license-free, quick deployment, and inherent security^[1-3]. However, the performance of FSO communications systems is mainly restricted by scattering and absorption losses and atmospheric-induced scintillation on the atmospheric transmission. In particular, the atmospheric turbulence effect is a major impairment of FSO systems^[4].

To alleviate atmospheric turbulence effects, pulse position modulation (PPM) is extensively employed in FSO communication systems^[5,6]. PPM is a type of signal modulation where a shift is made in the position of the pulse signal. In practical applications, two decoding algorithms can be used for the PPM signals. A decoding algorithm is hard decision decoding that uses a threshold detector, while the other one is soft decision decoding, which uses a maximum *a posteriori* or maximum likelihood detector^[7]. Owing to the bit error rate (BER) performance of soft decision decoding being superior to hard decision decoding, soft decision decoding is usually used in FSO communications^[4-6]. However, the soft decision decoding receivers are generally based on a field-programmable gate array (FPGA)^[8-10] or erbium-doped waveguide amplifier (EDWA) planar lightwave circuits (PLCs)^[11], which leads to its hardware being more complicated and more consumptive than the hard decision decoding receiver's.

With the growing needs of communication quality, the study of FSO communication is no longer confined to a single modulation technology. An effective technology to control error is using automatic repeat request (ARQ) in the FSO links^[12-17]. In these studies, specific theoretical analysis for ARQ systems are investigated, and the combination of ARQ and other technology

such as forward error correction [that is hybrid ARQ (HARQ)]^[12-14], the Rateless Round Robin protocol^[15], Luby Transform codes^[16], and adaptive-rate transmission^[17], are presented. These systems do not take modulations into account, especially PPM technology. Therefore, the more efficient and comprehensive hybrid scheme, which combines ARQ and PPM, has been considered. The combination of ARQ and PPM was first presented in Refs. [18,19], which have investigated the performance of infrared communication systems using repetition-rate coding and ARQ schemes over PPM wireless links throughout indoor environments. The scheme has the advantage that there is no need to use other error detecting codes in the data packet, and its drawback is a low throughput efficiency because each PPM symbol is repeated; in Ref. [20], a method used in infrared communication, which is the combination of SR-ARQ and repetition coded PPM, has been discussed. This system's characteristic is that it can dynamically change the link transmission rate according to the channel state. The scheme can be used in adverse channel conditions that are mentioned above. In Ref. [21], the HARQ technique that uses binary PPM for FSO communications over log-normal channels has been investigated. The HARQ protocol improves the error control performance and brings more complexity and overhead to the system at the same time. Furthermore, in Refs. [18-21], the whole packet must be retransmitted when the packet's parity check fails. In that case, the successfully decoded portion of the packet is still retransmitted, and it brings about the waste of communication resources.

Therefore, we propose to an HARQ-FSO communication system (hereinafter it is referred to as the ARQ-FSO system), which is a combination of a novel ARQ and PPM. The novel ARQ has the main characteristic

that the scheme does not need the parity-check code and only retransmits the failed decoded symbols of the packet. The error detecting way uses the decision result of each PPM symbol to detect errors without the error detecting code. The PPM symbol error detection is based on the characteristics of the PPM symbol, where a successfully decoded PPM symbol has just one pulse. If the decoded PPM symbol has no pulse or multiple pulses, the receiver will send those PPM symbols to the transmitter. Therefore, the ARQ-FSO system doesn't have the latency of the parity-check code's generation and verification. The selection of the retransmission data depends on the special negative acknowledgements (NACKs). The extra sequence numbers, which are the error PPM symbol's sequence indexes in the packet, are added in the NACKs of the novel ARQ. The transmitter only retransmits the corresponding PPM symbols instead of the whole packet. Considering the effect of the special NACKs' transmission time, the transmission and processing time of the proposed system are also less than the traditional ARQ, where the numbers of the error PPM symbols are less than half of the received packet's size. Thus, the proposed scheme has advantages in the latency and efficiency over the traditional ARQ.

In FSO communications, the turbulence effect is a main limitation factor. Atmospheric-induced scintillation causes random variations in signal intensity^[6]. Atmospheric turbulence is classified according to the magnitude of the index of refraction variation and inhomogeneity as weak, moderate, strong, and saturated. Under these turbulence conditions, various mathematical models, such as log-normal^[3,22], gamma-gamma^[2,23] and negative exponential^[3] distribution, are described as the probability density function (pdf) statistics of the irradiance fluctuation.

In this Letter, the weak turbulence circumstance is discussed and represented by the log-normal mathematical model. Therefore, the pdf of the received optical intensity is expressed as^[7]

$$f_I(I) = \frac{1}{I\sigma_I\sqrt{2\pi}} \exp\left\{-\frac{[\ln(I/I_0) + \sigma_I^2/2]^2}{2\sigma_I^2}\right\}, \quad (1)$$

where I represents the received optical intensity, and I_0 is the received average irradiance without atmospheric turbulence. σ_I^2 stands for the log-amplitude variance, which relies on the characteristics of the channel. If the receive signal is a plane wave, the log irradiance variance σ_I^2 is given by

$$\sigma_I^2 = 1.23 C_n^2 k^{7/6} L_p^{11/6}, \quad (2)$$

where C_n^2 denotes the refractive index structure coefficient. k is the optical wave number, and L_p is the distance.

The structure of the ARQ-FSO communication system is shown in Fig. 1. In this Letter, the parameter L of L -PPM is 256. The receiver uses the hard decision method.

In the communications of the ARQ-FSO system, the data is divided into fixed length packets as P , and P is

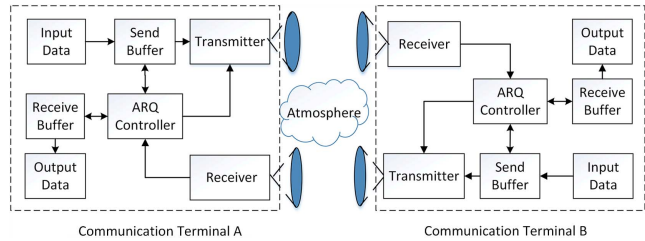


Fig. 1. Block diagram of ARQ-FSO communication systems.

an integer multiple of M ($M = \log_2 L$). Taking communication terminal A as an example, it describes and analyzes the communication steps for the ARQ-FSO system. First, the data are packed by communication terminal A as a number of fixed length packages. Next, these packages are stored in the send buffer and are modulated into PPM signals. Subsequently, the transmitter performs signals transmission via atmospheric turbulence channels. In communication terminal B, the received signals are decoded and demodulated by the receiver. On one hand, if the decoded PPM symbols are a single pulse, they are stored in the receive buffer. On the other hand, if the PPM fails to decode, the sequence numbers of the PPM symbols are modulated into PPM signals and sent to terminal A. Then, terminal A carries out the signal demodulation. According to the sequence numbers, the ARQ controller extracts the corresponding data from the send buffer and then transmits them out. It is not until either all received PPM symbols are successfully decoded or the number of retransmissions exceeds the maximum number will the communications be complete.

According to the mentioned channel model and system model, the received signal of the photoelectric detector can be given as^[24,25]

$$y = \eta Ix + n, \quad (3)$$

where y stands for the received signal, n denotes the additive white Gaussian noise and $n \sim N(0, N_0/2)$. η indicates the effective photo-current conversion ratio of the receiver, and I expresses the normalized irradiance. x is the PPM symbol sequence.

In the log-normal channel, the random parameter I is treated as the constant at an instant. The probability of a slot error for the direct hard decoding at an instant can be expressed as^[26]

$$P_{\text{slot error}} = P(0)Q\left(\frac{\alpha_T}{\sqrt{N_0/2}}\right) + P(1)Q\left(\frac{I\sqrt{E_S} - \alpha_T}{\sqrt{N_0/2}}\right), \quad (4)$$

where $Q(x)$ is $0.5\text{erfc}(x/\sqrt{2})$, and α_T stands for the threshold level. E_S represents the average energy per symbol. $P(0)$ and $P(1)$ are the probabilities of $c_k = 0$, and $c_k = 1$, respectively, which are described by $P(1) = 1/L$, and $P(0) = 1 - P(1)$.

Based on Eqs. (1) and (4) and the pdf of I , the probability of the slot error of the direct hard decoding can be calculated as

$$P_{\text{sle}_H} = \int_0^\infty f_I(I) P_{\text{sle}_H-t} dI. \quad (5)$$

According to the following Gauss–Hermite formula^[27], where α_T is assumed $0.5I\sqrt{E_b}$, Eq. (5) can be approximated and simplified as

$$P_{\text{sle}_H} = \frac{1}{\sqrt{\pi}} \sum_{i=1}^m w_i Q \left[\sqrt{\frac{E_b M}{2N_0}} I_0 \exp \left(\sqrt{2\sigma_i^2} x_i - \frac{\sigma_i^2}{2} \right) \right], \quad (6)$$

where w_i and x_i stand for the weight factors and the zeros of the Hermite polynomial, respectively. E_b represents the average energy per bit, and M equals $\log_2 M$.

Owing to the PPM symbol having L slots, the probability of the symbol error is derived through the corresponding slot error probability and is expressed as

$$P_{\text{sy}_e_H} = 1 - (1 - P_{\text{sle}_H})^L. \quad (7)$$

The probability of the symbol error of the direct soft decoding is given as^[7]

$$P_{\text{sy}_e_S} = \frac{1}{\sqrt{2\pi}} \int_{-\infty}^{\infty} \int_0^\infty f_I(I) [1 - (1 - Q(y))^{L-1}] \times \exp \left[-0.5 \left(y - \sqrt{\frac{2ME_b}{N_0}} I \right)^2 \right] dy dI. \quad (8)$$

Assuming the data are independently and identically distributed (IID), the BER is calculated through the corresponding symbol error probability and is given as^[28]

$$P_{\text{ber}} = \frac{L/2}{L-1} P_{\text{sy}_e}. \quad (9)$$

In the ARQ-FSO system, it is difficult to directly solve the BER. Thus, we can first derive the probability of the symbol correctly. The received PPM symbol has only a pulse when the received symbol is successfully decoded. At this point, we assume that the probability of the received single pulse in the PPM symbol, which is sent by one pulse, is P_{E1} , and empty is P_{E0} . It can be derived as

$$P_{E1} = \int_0^\infty f_I(I) \left[1 - Q \left(I \sqrt{\frac{E_b M}{2N_0}} \right) \right]^L dI, \quad (10)$$

$$P_{E0} = \int_0^\infty f_I(I) (L-1) Q \left(I \sqrt{\frac{E_b M}{2N_0}} \right)^2 \left[1 - Q \left(I \sqrt{\frac{E_b M}{2N_0}} \right) \right]^{L-2} dI. \quad (11)$$

Therefore, the probability of the received PPM symbols, which need no retransmission, is $P_E (P_E = P_{E0} + P_{E1})$. At the i th retransmission, the probability of the symbol being correct in the receiver is improved and can be computed as

$$S_i = (1 - P_E)^i (1 - P_{\text{sy}_e_H}) P_{E1}. \quad (12)$$

Based on the sum formula of the geometric sequence and Eq. (12), the probability of the correct symbol after i retransmissions is described by

$$P_{\text{sync_ARQ}} = P_{E1} + \frac{P_{E1}(1 - P_E)(1 - P_{\text{sy}_e_H})[1 - (1 - P_E)^i]}{P_E}. \quad (13)$$

According to Eq. (9), the probability of the correct symbol can be converted into a corresponding BER using

$$P_{\text{ber_ARQ}} = \frac{L/2}{L-1} (1 - P_{\text{sync_ARQ}}). \quad (14)$$

Optimally, the received PPM symbol is all successfully decoded after repeated retransmission. At this moment, the optimal BER can be approximated and given by

$$P_{\text{ber_ARQ_optimal}} = \frac{L/2}{L-1} \left[\frac{P_{E0} + P_{E1}(1 - P_E) P_{\text{sy}_e_H}}{P_E} \right]. \quad (15)$$

The throughput efficiency is the ratio of the bit number of the successfully decoded symbols in the receiver and the sum of the transmitted bits in the transmitter, which is one of the important indexes of the ARQ system. In the traditional selective repeat (SR) ARQ systems, the throughput efficiency can be derived as^[29]

$$\eta_{\text{SR_ARQ}} = P_c R = (1 - P_{\text{ber}})^n \frac{k}{n}, \quad (16)$$

where P_c is the probability of the received packet that contains no error, and can be computed by the system BER. R stands for the code rate and is the ratio of information bits k and total input bits n . Based on the characteristics of the ARQ-FSO system and the definition of the throughput efficiency, the throughput efficiency of the ARQ-FSO system can be expressed as

$$\eta_{\text{ARQ_FSO}} = P_{\text{sync}} P_E. \quad (17)$$

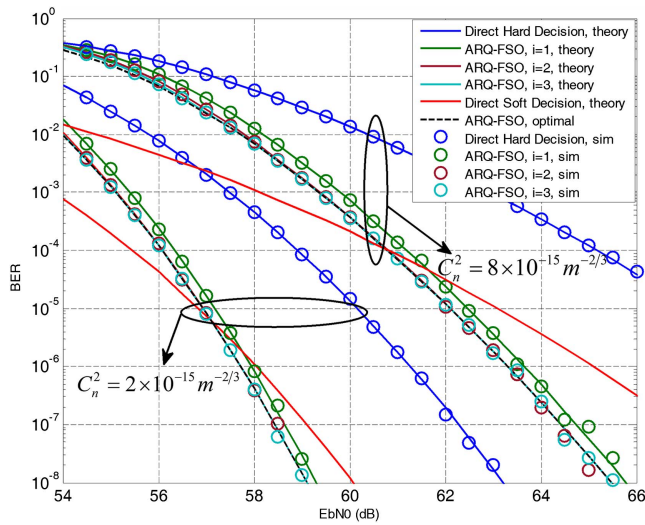


Fig. 2. BER versus E_b/N_0 for the ARQ-FSO system and direct decision under different turbulence strengths.

Then, the BER performance of the ARQ-FSO system in the log-normal channel is simulated and compared with the direct hard decision system and the direct soft decision system. The wavelength of the lasers is 1550 nm, and the effective photo-current conversion ratio of the receiver is idealized and assumed as one.

First, Fig. 2 depicts the BER for the ARQ-FSO system compared with the direct hard decision system and the direct soft decision system over different turbulence strengths ($c_n^2 = 8 \times 10^{-15} \text{ m}^{-2/3}$, $c_n^2 = 2 \times 10^{-15} \text{ m}^{-2/3}$). It is seen that the simulated and measured results are in good agreement with each other and show that this theoretical analysis is correct. Meanwhile, the BER performance of the direct hard decision system is significantly improved by using the ARQ-FSO scheme, which is better than the direct soft decision system in most cases. For instance, we select the same parameters, where the ratio of bit energy to noise power (E_b/N_0) is 64 dB, and $c_n^2 = 8 \times 10^{-15} \text{ m}^{-2/3}$. The BER of the ARQ-FSO system are declined to 5×10^{-7} and 1×10^{-8} under conditions that the maximum numbers of retransmission i are one and three, respectively, while the direct hard decision system and the direct soft decision system are just 5×10^{-4} and 5×10^{-6} . At $c_n^2 = 8 \times 10^{-15} \text{ m}^{-2/3}$, to achieve 1×10^{-6} of the BER, the requested E_b/N_0 of the direct hard decision system and the direct soft decision system are well over 66 and 65 dB, but the ARQ-FSO system is only 63.5 dB when the maximum number of retransmission is three. Compared with the direct hard decision system and the direct soft decision system, the ARQ-FSO system separately obtains about the 6.5 and 1.5 dB gain. At $c_n^2 = 2 \times 10^{-15} \text{ m}^{-2/3}$, the required E_b/N_0 to achieve the same BER as the above ARQ-FSO system with the maximum number of retransmission of three is 3.5 dB lower than that just using the hard decision. Based on the above analysis, we find that the PPM system BER performance is noticeably improved

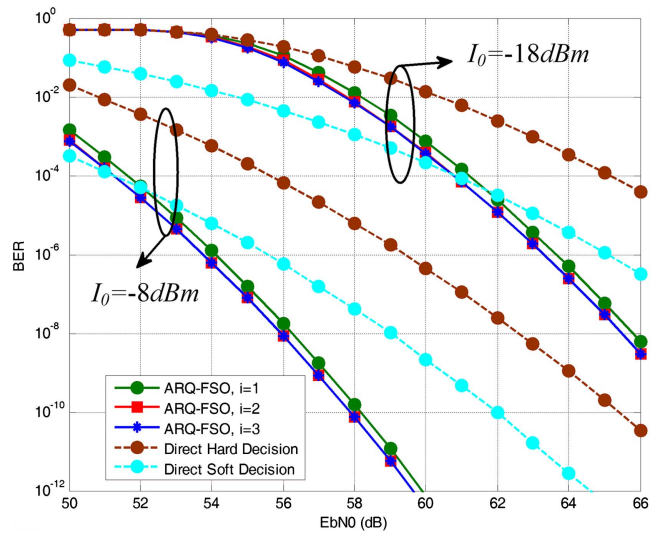


Fig. 3. BER versus E_b/N_0 for different I_0 with $c_n^2 = 8 \times 10^{-15} \text{ m}^{-2/3}$.

by using the proposed ARQ scheme over turbulence channels, and when the turbulence strengths are stronger, the ameliorated effect is more obvious.

Next, in Fig. 3, the BER is discussed versus E_b/N_0 for the ARQ-FSO system and direct decision systems for different I_0 with $c_n^2 = 8 \times 10^{-15} \text{ m}^{-2/3}$. When $E_b/N_0 = 60$ dB and $I_0 = -18$ dBm, the BER of the direct hard decision system is merely 1×10^{-2} . The performance shows less difference between the direct soft decision system and the ARQ-FSO system with the maximum number of retransmission of three, and it is about 1×10^{-4} . Then, at the same E_b/N_0 , if $I_0 = -8$ dBm, the BER performance of the direct hard decision system and the direct soft decision system approach 1×10^{-6} and 1×10^{-9} , and ARQ-FSO system with the maximum number of retransmission of three almost reaches 1×10^{-12} . We can clearly observe that the augment of the received average irradiance I_0 leads to the decline of the BER performance, and the system has marked improvement by using the ARQ over the turbulence channels. Based on the above analysis, we can find that it is important to choose the appropriate parameter of I_0 in the ARQ-FSO system.

The BER performance versus link distance for the ARQ-FSO system and direct decision systems is investigated in Fig. 4. We fix $c_n^2 = 2 \times 10^{-15} \text{ m}^{-2/3}$, and $E_b/N_0 = 58$ dB. It can also be seen from the figure that the BER performance of the ARQ-FSO system is superior to the direct hard decision system and the direct soft decision system. For example, when the link distance $L_P = 2000$ m, the BER of the direct hard decision system and the direct soft decision system are only 1×10^{-6} and 1×10^{-8} , respectively. The ARQ-FSO system with the maximum number of retransmission of three declines to 1×10^{-11} . Meanwhile, the increasing of the link distance would weaken the BER performance of the ARQ-FSO system, and the performance's advantages become less obvious. The causes for these results are that the increase of link distance brings

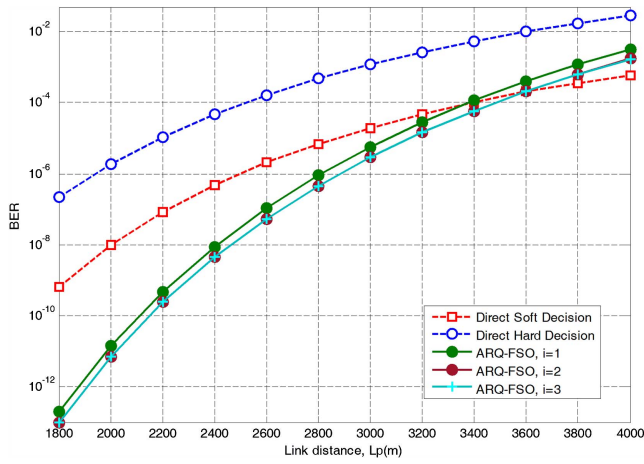


Fig. 4. BER versus link distance for the ARQ-FSO system and direct decision with $c_n^2 = 2 \times 10^{-15} \text{ m}^{-2/3}$.

about the growth of the log intensity variance σ_I^2 , and then the BER performance gets worse. According to Figs. 2, 3, and 4, we can see that the ARQ-FSO system with the maximum number of retransmission of three can achieve the desired performance.

Finally, Fig. 5 illustrates the throughput efficiency against E_b/N_0 for the ARQ-FSO system and two SR-ARQ systems with $c_n^2 = 8 \times 10^{-15} \text{ m}^{-2/3}$, and $I_0 = -18 \text{ dBm}$. It is found that the throughput performance of the ARQ-FSO system is always superior to the traditional SR-ARQ systems no matter what kind of PPM decoding the traditional SR-ARQ systems use. When the throughput efficiency is 0.7, the required E_b/N_0 to achieve the throughput efficiency of the ARQ-FSO system is 8 and 4 dB, which is reduced more than the SR-ARQ systems using PPM hard decision and PPM soft decision, respectively.

In conclusion, we present an innovative hybrid wireless optical communication system called the ARQ-FSO

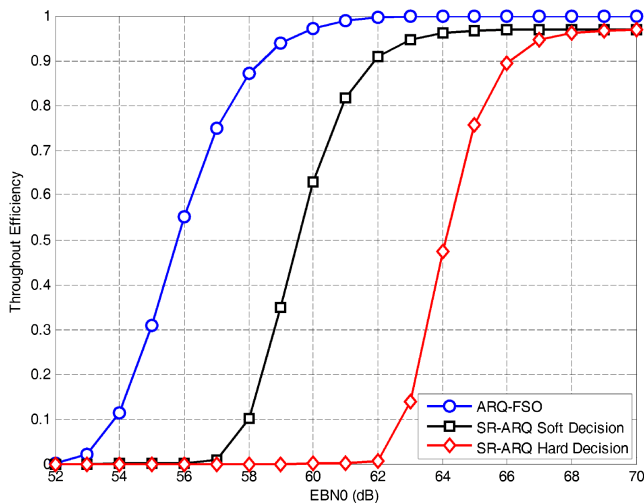


Fig. 5. Throughput efficiency versus E_b/N_0 for the ARQ-FSO system and two SR-ARQ systems with $c_n^2 = 8 \times 10^{-15} \text{ m}^{-2/3}$, and $I_0 = -18 \text{ dBm}$.

system, according to the characteristics of FSO communication and the hardware peculiarity of the PPM decision, which combines the PPM hard decision with a novel ARQ and depends on the PPM hard decision results to detect data errors. The BER and the throughput efficiency of the proposed system are investigated over weak atmospheric turbulence channels. The numerical results demonstrate that the BER performance of the direct hard decision system is significantly improved by using the proposed ARQ scheme. Then, the desired performance of this system can be achieved by less times of retransmission. Moreover, we find that the ARQ-FSO system has the superior BER performance under the not extremely bad channel conditions, and it remarkably selects the appropriate parameter I_0 of the ARQ-FSO system. Additionally, the average throughput efficiency of the proposed system is superior to the traditional ARQ systems.

This work was supported by the National Natural Science Foundation of China (No. 61475049) and the National Basic Research Program of China (No. 2013CB29204).

References

1. M. A. Khalighi and M. Uysal, *IEEE Commun. Surv. Tut.* **16**, 2231 (2014).
2. T. Cao, P. Wang, L. Guo, B. Yang, J. Li, and Y. Yang, *Chin. Opt. Lett.* **13**, 080101 (2015).
3. M. Abaza, R. Mesleh, A. Mansour, and E. Aggoune, *Chin. Opt. Lett.* **13**, 051001 (2015).
4. X. M. Zhu and J. M. Kahn, *IEEE. Trans. Commun.* **50**, 1293 (2002).
5. P. Wang, J. Qin, L. Guo, and Y. Yang, *IEEE. Photon. Technol. Lett.* **28**, 252 (2016).
6. K. Kiasaleh, *IEEE. Trans. Commun.* **53**, 1455 (2005).
7. Z. Ghassemlooy, W. Popoola, and S. Rajbhandari, *Optical Wireless Communications: System and Channel Modelling with MATLAB* (CRC Press, 2012).
8. S. Karp and R. M. Gagliardi, *IEEE. Trans. Commun. Technol.* **17**, 670 (1969).
9. S. B. Baiguanysh, A. B. Mirmanov, A. S. Alimbaev, and A. Y. Makartseva, in *2015 International Siberian Conference on Control and Communications* (2015), p. 4.
10. X. Fu, G. Chen, T. Tang, Y. Zhao, P. Wang, and Y. Zhang, in *2010 Symposium on Photonics and Optoelectronics* (2010), p. 1.
11. A. J. Mendez, V. J. Hernandez, R. M. Gagliardi, and C. V. Bennett, in *2009 IEEE Leos Annual Meeting Conference Proceedings, Vols. 1 and 2* (2009).
12. S. M. Aghajanzadeh and M. Uysal, *IEEE. Trans. Commun.* **60**, 1432 (2012).
13. E. Zedini, A. Chelli, and M. S. Alouini, *IEEE. Photon. J.* **6**, 1 (2014).
14. S. Parthasarathy, A. Kirstaedter, and D. Giggenbach, in *Photonic Networks; 17. ITG-Symposium* (2016), p. 1.
15. A. R. Hammons and F. Davidson, in *Military Communications Conference* (2010), p. 808.
16. G. Prakash, A. Nayak, M. Kulkarni, and S. Acharya, in *2013 IEEE 16th International Conference on Computational Science and Engineering* (2013), p. 1195.
17. V. V. Mai and A. T. Pham, *IEEE. Photon. J.* **8**, 1 (2016).
18. T. Ozugur, M. Naghshineh, P. Kermani, C. M. Olsen, B. Rezvani, and J. A. Copeland, in *1998 The Ninth IEEE International*

- Symposium on Personal, Indoor and Mobile Radio Communications* (1998), p. 698.
19. T. Ozugur, M. Naghshineh, P. Kermani, and J. A. Copeland, *Int. J. Commun. Syst.* **13**, 617 (2000).
 20. K. Samaras, D. C. O'Brien, and D. J. Edwards, *Electron. Lett.* **34**, 2199 (1998).
 21. K. Kiasaleh, *IEEE. Commun. Lett.* **14**, 866 (2010).
 22. Y. Y. Zhang, H. Y. Yu, J. K. Zhang, and Y. J. Zhu, *Opt. Express* **24**, 7905 (2016).
 23. C. Liu, Y. Yao, Y. Sun, and X. Zhao, *Chin. Opt. Lett.* **8**, 537 (2010).
 24. J. Li and M. Uysal, in *2003 IEEE 58th Vehicular Technology Conference* (2003), p. 168.
 25. H. G. Sandalidis and T. A. Tsiftsis, *Electron. Lett.* **44**, 46 (2008).
 26. J. R. Barry, *Wireless Infrared Communications* (Kluwer Academic, 1994).
 27. D. B. Owen, *Technometrics* **7**, 78 (1965).
 28. J. G. Proakis and M. Salehi, *Digital Communications* (McGraw-Hill, 2008).
 29. S. Lin, D. J. Costello, Jr., and M. J. Miller, *IEEE. Commun. Mag.* **22**, 5 (1984).